

Gamma-Ray Lines from Asymmetric Supernovae

A. L. HUNGERFORD^a, C. L. FRYER^b, AND M. S. WARREN^b

^aLos Alamos National Laboratory, Transport Methods Group CCS-4, Los Alamos, NM 87545, USA

^bLos Alamos National Laboratory, Theoretical Astrophysics Group T-6, Los Alamos, NM 87545, USA

ABSTRACT

We present simulations of supernova explosions in 3-dimensions, from 100s to 1 year after core-bounce. A series of initial explosion conditions, with both jet-like “axial” and equatorial asymmetries of varying degree, were modeled (guided by the simulations of Fryer & Heger 2000). These simulations and their results are compared with past work. A post-processing analysis of the γ -ray emission in these models was conducted, using a 3D Monte Carlo γ -ray transport code. The γ -ray spectra calculated are presented as a function of time since the explosion and viewing angle of the ejecta.

1 Background

Among the many surprises that supernova (SN) 1987A brought astronomers was the early emergence of X-ray and γ -ray emission (X-rays e.g. [6], [25]; γ -rays: e.g. [5], [15], [16]). This high energy emission, arising from the decay of ^{56}Co , appeared nearly 6 months earlier than was predicted by theoretical models (see Figure 1) and led theorists to conclude that the ^{56}Ni , produced deep in the core of this exploding star, had mixed into the outer layers of the supernova ejecta ([21], [3] and references therein). Observations of other supernovae seem to suggest that SN 1987A is not peculiar in this mixing. Many supernovae show evidence of mixing in their spectra (e.g. [24], [7]) and the light curves and spectra of Type Ib SNe seem to be best fit by mixed models ([22], [28]). It appears that mixing is a generic process in core-collapse supernovae.

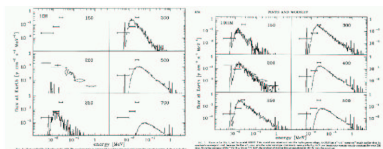


Figure 1. Spectrally corrected models of the γ -ray emission from SN 1987A. Left panel is for an explosion model of progenitor 1997 with no mixing. Right panel is for an explosion of the same progenitor model, but where efficient outward mixing of the ^{56}Ni has been included. It is clear that including the effects of mixing greatly improves the theoretical fit to observed data.

These observational results have stimulated a series of multi-dimensional hydrodynamical simulations trying to produce the observed mixing ([2], [10], [9], [17], [11], [12], [13], [14]). Although these simulations seem to be able to explain the mixing in Type Ib supernovae ([14]), none of these results are able to explain the extensive mixing observed in SN 1987A. Possible solutions are that the decay of ^{56}Ni injects enough energy to force additional mixing ([12]) or perhaps convection in the pre-collapse core provides enough seeds to enhance mixing ([12]). A third possibility is that the supernova explosion itself is asymmetric ([18], [19], [20] and references therein). Nagataki et al. (1998) found that slight asymmetries in the supernova explosion could not only produce the required mixing to explain 1987A, but they could also explain anomalies in the nucleosynthetic yields produced by several supernovae. In this work, we have combined hydrodynamical modelling efforts of 3-dimensional supernova explosions, with Monte Carlo gamma-ray transport simulations. We use these combined models to investigate trends in the emergent γ -ray spectra due to asymmetries imparted in the explosion mechanism.

References

- [1] Ambwani, K. & Sutherland, P. 1988, *ApJ*, 325, 820
- [2] Arnett, D., Fryxell, B., & Müller, E. 1989, *ApJ*, 341, L63
- [3] Arnett, W. D., Bahcall, J. N., Kirshner, R. P., & Woosley, S. E. 1989, *ARA&A*, 27, 629
- [4] Chevalier, R. A., & Klein, R. I. 1978, *ApJ*, 269, 281
- [5] Cook, W. R., Palmer, D. M., Prince, T. A., Schindler, S. M., Starr, C. H., & Stone, E. C. 1988, *ApJ*, 334, L87
- [6] Dotani, T., Hayashida, K., Inoue, H., Itoh, M., & Koyama, K. 1987, *Nature*, 330, 230
- [7] Fassia, A., Meikle, W. P. S., Geballe, T. R., Walton, N. A., Pollacco, D. L., Rutten, R. G. M., Tinney, C. 1998, *MNRAS*, 299, 150
- [8] Fryer, C. L., & Heger, A. 2000, *ApJ*, 541, 1033
- [9] Fryxell, B., Arnett, D., & Müller, E. 1991, *ApJ*, 367, 619
- [10] Hachisu, I., Matsuda, T., Nomoto, K., & Shigeyama, T. 1990, *ApJ*, 358, L57
- [11] Herant, M., & Benz, W. 1991, *ApJ*, 370, L81
- [12] Herant, M., & Benz, W. 1992, *ApJ*, 387, 294
- [13] Herant, M., & Woosley, S. E. 1994, *ApJ*, 425, 814
- [14] Kifonidis, K., Plewa, T., Janka, H.-Th., Müller, E. 2000, *ApJ*, 531, L123
- [15] Mahoney, W. A., Varnell, L. S., Jacobson, A. S., Ling, J. C., Radcinski, R. G., & Wheaton, Wm. A. 1988, *ApJ*, 334, L81
- [16] Matz, S. M., Share, G. H., Leising, M. D., Chupp, E. L., & Vestrand, W. T. 1988, *Nature*, 331, 416
- [17] Müller, E., Fryxell, B., & Arnett, D. 1991, *A&A*, 251, 505
- [18] Nagataki, S., Hashimoto, M., Sato, K., & Yamada, S. 1997, *ApJ*, 486, 1026
- [19] Nagataki, S., Shimizu, T.M., & Sato, K. 1998, *ApJ*, 495, 413
- [20] Nagataki, S. 2000, *ApJS*, 127, 141
- [21] Pinto, P. A., & Woosley, S. E. 1988, *ApJ*, 329, 820
- [22] Shigeyama, T., Nomoto, K., Tsujimoto, T., & Hashimoto, M. 1990, *ApJ*, 361, L23
- [23] Spyromilio, J., Meikle, W. P. S., & Allen, D. A. 1990, *MNRAS*, 242, 669
- [24] Spyromilio, J. 1994, *MNRAS*, 266, L61
- [25] Sunyaev, R., Kaniovskii, A., Efremov, V., Gilfanov, M., & Churazov, E. 1987, *Nature*, 330, 227
- [26] Weaver, T. A., & Woosley, S. E. 1980, in *AIP Conf. Proc. 63, Supernovae Spectra*, ed. R. Meyerott & G. H. Gillespie (New York: AIP), 15
- [27] Weaver, T. A., & Woosley, S. E. 1993, *Phys. Rep.*, 227, 65
- [28] Woosley, S. E., & Eastman, R. G., 1997, in *Thermonuclear Supernovae*, Proceedings of the NATO Advanced Study Institute, Begur, Girona, Spain, June 20-30, 1995, Dordrecht: Kluwer Academic Publishers, 1997, edited by P. Ruiz-Lapuente, R. Canal, and J. Isern. NATO Advanced Science Institutes (ASI) Series C, Volume 486, p.821

2 SPH Explosion Simulations

2.1 Highlights

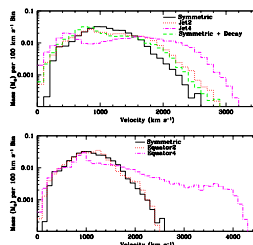


Figure 2. Mass of ^{56}Ni versus velocity of ejecta for the different initial explosion conditions in a 15 M_{\odot} red super giant progenitor star. Including the decay energy or global asymmetries in the explosion serves to enhance the outward mixing of the ^{56}Ni at the 15% or higher level.

2.2 Jet2 and Symmetric Models

For our hydrodynamic simulations, we have used the 15 M_{\odot} progenitor (s15s7b) by Weaver & Woosley (1993). This star has been evolved with a piston-driven explosion to 100s after bounce. The total energy of this model is roughly 1.5×10^{51} erg with roughly 1.0×10^{51} erg in kinetic energy. As this explosion moves through the star, the shock hits composition boundaries where strong entropy gradients exist. When the shock hits these boundaries (especially the helium-hydrogen interface), Rayleigh-Taylor instabilities develop, which can grow and cause the star to mix (Chevalier & Klein 1978; Weaver & Woosley 1980). Our simulations model this mixing and concentrate on the effects that asymmetries have on this mixing. As can be seen in the ^{56}Ni distribution plots above, a jet-like axial explosion with aspect ratio 2:1 serves to enhance the outward mixing of heavier elements from maximum ejecta velocities of $\sim 2500 \text{ km s}^{-1}$ to 2000 km s^{-1} . It is interesting to note that including the effects of the ^{56}Ni decay energy injection enhances the mixing by a similar amount. This seemingly small effect on the velocity distribution of decay products, results in rather significant changes in the observed γ -ray emission (see Section 3).

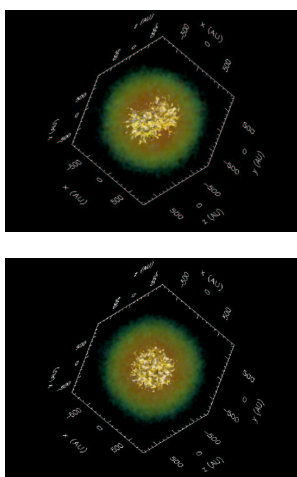


Figure 3. A 3-dimensional rendering of the explosion density (the background color) and ^{56}Ni number density (the solid body surface) distribution at $t = 1$ year after explosion for both the Jet2 (top) and Symmetric (bottom) models. The density structure of the ejecta remains roughly spherical while the heavy element distribution (as demonstrated here by the ^{56}Ni) reflects the 2:1 asymmetry imparted during the explosion.

3 Monte Carlo γ -ray Spectra

3.1 Highlights

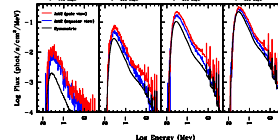


Figure 4. Emergent hard X-ray emission is more than ~ 2 times brighter for the Jet2 asymmetric explosion (regardless of viewing angle) than for the Symmetric explosion. In addition, the γ -ray line fluxes for the Jet2 model are more than ~ 4 times higher than in the Symmetric explosion model.

3.2 Line Profiles

We used a Monte Carlo technique, similar to that described in Ambwani & Sutherland 1987, for modelling the γ -ray transport in 3-dimensions. Input models of the supernova ejecta (element abundances, density and velocities) were taken from the SPH explosion simulations (models Jet2 and Symmetric) and mapped onto a $140 \times 140 \times 140$ cartesian grid. Escaping photons were tallied into energy and angular bins for 4 different snapshots in time of the supernova evolution. Regardless of viewing angle, the asymmetric Jet2 explosion produces a brighter flux across the entire high energy spectrum (see Figure 4). The ^{56}Co line emission at 1.238 and 0.847 MeV from ^{56}Ni decay shows blue-shifted line profiles whose centroids shift rearward with the time since explosion. As the supernova expands, emission from material located deeper into the ejecta (and thus at smaller radial velocities) becomes visible, resulting in the observed rearward shift of the line center. In addition, variations in the line profiles with viewing angle are only present for the asymmetric (Jet2) explosion model, as one would expect. The blue edge to the lines (top panel of Figure 5) are dictated by the maximum observed radial velocity of the ^{56}Co in the ejecta, which is an indication of the extent to which the heavy elements were mixed outward in the explosion. We see that the blue edge of the lines shift to lower velocities as we look from pole to equator views, indicating that outward mixing is more vigorous along the direction of the imparted explosion asymmetry. The red edge to the lines is determined by the escaping emission from ^{56}Co with the smallest velocity in the ejecta. Since there are fewer heavy elements injected into the equatorial angle, the optical depth to bound-free absorption is smaller along this view and we are able to see deeper into the ejecta, thus probing the smaller ejecta velocities. This results in a line profile with a red edge further rearward for angles closer to the equator, as is seen in the calculated spectrum for the Jet2 explosion.

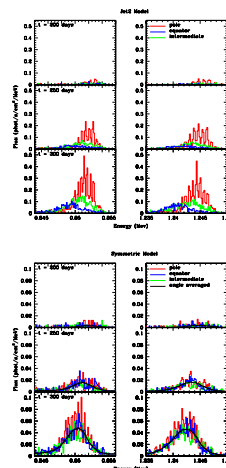


Figure 5. 1.238 and 0.847 MeV line profiles as a function of time during the explosion. Top panel shows line profiles for different viewing angles of the Jet2 model. Bottom panel shows line profiles for different viewing angles of the Symmetric model. The fluxes are offset by a factor of 2 between the Jet2 and Symmetric models. For all viewing angles the Jet2 explosion produces a higher flux in these γ -ray lines than does the Symmetric explosion. The bottom panel demonstrates that the line profiles do not vary significantly with viewing angle for the Symmetric model and the higher 1/4 angle averaged line profile for this model is also plotted.